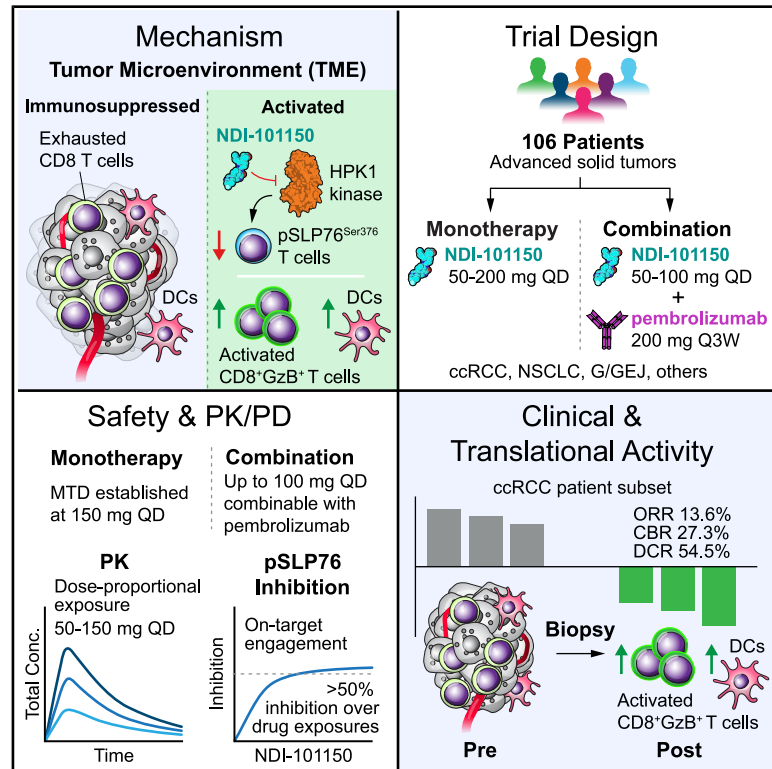


# HPK1 inhibitor NDI-101150 as monotherapy and in combination with pembrolizumab in patients with advanced solid tumors: Phase 1/2 trial results

## Graphical abstract



## Authors

David A. Braun, Marcus S. Noel, Ryan H. Moy, ..., Pavan Kumar, Anita Scheuber, David Sommerhalder

## Correspondence

david.braun@yale.edu (D.A.B.), anita.scheuber@nimbustx.com (A.S.)

## In brief

Braun et al. report a phase 1/2 study evaluating NDI-101150, a potent, selective HPK1 inhibitor in patients with advanced solid tumors. NDI-101150 shows favorable safety as a monotherapy or in combination with pembrolizumab, with monotherapy demonstrating on-target immune activation and durable responses in patients with clear cell renal cell carcinoma.

## Highlights

- NDI-101150 is a potent, selective oral HPK1 inhibitor dosed once daily
- Phase 1/2 human trial in advanced solid tumors as monotherapy and with pembrolizumab
- Favorable tolerability and combinability with pembrolizumab in heavily pretreated patients
- Monotherapy efficacy in clear cell RCC, with expected pharmacodynamic effects observed

## Article

# HPK1 inhibitor NDI-101150 as monotherapy and in combination with pembrolizumab in patients with advanced solid tumors: Phase 1/2 trial results

David A. Braun,<sup>1,18,\*</sup> Marcus S. Noel,<sup>2</sup> Ryan H. Moy,<sup>3</sup> Kurt Demel,<sup>4</sup> Martin Gutierrez,<sup>5</sup> Sunil Sharma,<sup>6</sup> Arif Hussain,<sup>7</sup> Shirish Gadgeel,<sup>8</sup> Julio Peguero,<sup>9</sup> Toni K. Choueiri,<sup>10,11</sup> Hamid Emamekhoo,<sup>12</sup> Brian Van Tine,<sup>13,17</sup> Rama Balaraman,<sup>14</sup> GiNell Elliott,<sup>15</sup> Sritama Nath,<sup>15</sup> Scott R. Daigle,<sup>15</sup> Pavan Kumar,<sup>15</sup> Anita Scheuber,<sup>15,\*</sup> and David Sommerhalder<sup>16</sup>

<sup>1</sup>Yale School of Medicine, New Haven, CT, USA

<sup>2</sup>Georgetown University Medical Center – Lombardi Comprehensive Cancer Center, Washington, DC, USA

<sup>3</sup>Columbia University Irving Medical Center, New York, NY, USA

<sup>4</sup>HealthPartners, St. Louis Park, MN, USA

<sup>5</sup>Hackensack University Medical Center – John Theurer Cancer Center, Hackensack, NJ, USA

<sup>6</sup>Honor Health Research Institute, Scottsdale, AZ, USA

<sup>7</sup>University of Maryland Greenebaum Comprehensive Cancer Center, Baltimore, MD, USA

<sup>8</sup>Henry Ford Cancer Institute, Henry Ford Health Center, Detroit, MI, USA

<sup>9</sup>Oncology Consultants, Houston, TX, USA

<sup>10</sup>Department of Medical Oncology, Dana-Farber Cancer Institute, Boston, MA, USA

<sup>11</sup>Harvard Medical School, Boston, MA, USA

<sup>12</sup>University of Wisconsin Carbone Cancer Center, Madison, WI, USA

<sup>13</sup>Department of Medicine, Division of Medical Oncology, Washington University in St. Louis, St. Louis, MO, USA

<sup>14</sup>Florida Cancer Affiliates-US Oncology, Ocala, FL, USA

<sup>15</sup>Nimbus Therapeutics, Boston, MA, USA

<sup>16</sup>NEXT Oncology, San Antonio, TX, USA

<sup>17</sup>Deceased

<sup>18</sup>Lead contact

\*Correspondence: [david.braun@yale.edu](mailto:david.braun@yale.edu) (D.A.B.), [anita.scheuber@nimbustx.com](mailto:anita.scheuber@nimbustx.com) (A.S.)

<https://doi.org/10.1016/j.xcrm.2026.102789>

## SUMMARY

Hematopoietic progenitor kinase 1 (HPK1) induces potent anti-tumor immunity in preclinical models by activating and recruiting T cells, B cells, and dendritic cells into the tumor microenvironment (TME). Here, we evaluate NDI-101150, a potent, selective HPK1 inhibitor, in a phase 1/2 trial as a monotherapy or in combination with pembrolizumab in patients with advanced solid tumors. The monotherapy maximum tolerated dose (MTD) is 150 mg once daily, and doses tested up to 100 mg once daily are combinable with pembrolizumab without reaching an MTD. In clear cell renal cell carcinoma, the investigator-assessed overall response rate with monotherapy treatment is 13.6%, including one complete response and two partial responses, with a clinical benefit rate of 27.3% and a disease control rate of 54.5%. Pharmacodynamic analyses show pharmacodynamic biomarker phospho-SLP76 inhibition and increased activated CD8<sup>+</sup> T cells and dendritic cells in the TME, supporting continued development (clinical registration number NCT05128487).

## INTRODUCTION

Immune CPIs, including antibodies targeting programmed cell death protein 1 (PD-1), its ligand programmed cell death ligand 1 (PD-L1), and cytotoxic T-lymphocyte-associated antigen 4 (CTLA-4), have substantially improved clinical outcomes in patients with advanced solid tumors. These therapies work by enhancing T cell functions, either by amplifying effector cell activity or by increasing the size and diversity of anti-tumor T cell populations.<sup>1–6</sup> Despite their transformative impact, responses to CPIs are limited to a subset of patients<sup>7,8</sup> and can often lack durability due to defined immune resistance archetypes.<sup>9</sup> For

example, in patients with advanced renal cell carcinoma (RCC), most patients experience disease progression on first-line CPIs.<sup>10–13</sup> It is proposed that the TME changes to a more immunosuppressed state, including loss of sufficient and suitable antigens, dysfunctional T cells, and lack of TME inflammation, to render these tumors resistant to CPI.<sup>14–18</sup> These challenges underscore the need for immunomodulatory therapies with mechanisms of action to overcome immunosuppression and deepen and extend clinical responses.

HPK1 is a serine/threonine kinase and member of the MAP4K family, a group of proteins that regulate physiological processes such as cellular signal transduction, including immune

responses.<sup>19</sup> HPK1 acts as a key intracellular regulator, functioning predominantly as a negative feedback modulator following T cell, B cell, and dendritic cell (DC) receptor stimulation.<sup>19–21</sup> Upon T cell and B cell receptor stimulation, HPK1 phosphorylates key adaptor proteins, SLP76 (on serine 376) in T cells and BLNK (on threonine 152) in B cells, leading to destabilization and attenuation of the downstream activation cascades.<sup>22–27</sup> Although not as well understood at a molecular level, HPK1 has also been shown to modulate DC activation.<sup>28</sup> Genetic knockout studies have demonstrated that loss of *hpk1* leads to T cell activation even under various immunosuppressive environments, including overexpression of prostaglandin E2 (PGE2), T cell exhaustion, and T regulatory cells<sup>29,30</sup> that are often characteristic of patients' TMEs that have progressed on prior CPIs.<sup>14–16</sup> This highlights the potential of HPK1 inhibition as a pharmacological mechanism to promote anti-tumor activity in this environment. Consistent with the proposed mechanism of action, *hpk1* knockout mice exhibit enhanced T cell infiltration into the tumor that is correlated with diminished growth of a variety of implanted syngeneic tumor cells.<sup>21,31</sup>

While genetic knockout studies establish HPK1 as a compelling target for cancer immunotherapy, one of the biggest hurdles in developing an effective HPK1 inhibitor has been identifying agents that are potent against and highly selective for HPK1 while not impacting other MAP4K family members. Selectivity is crucial for this approach, because while HPK1 is a negative regulator of immune cell activation, closely related mitogen-activated protein kinase kinase kinase (MAP4K) family members have the opposite effect. One notable example is germinal center kinase-like kinase (GLK), which transduces receptor-mediated signals that promote immune cell activation.<sup>32</sup> Therefore, a small molecule that inhibits GLK with similar potency as HPK1 would dampen immune cell activation, effectively canceling out HPK1 inhibition and its ability to enhance anti-tumor immune cell responses. NDI-101150, a potent small molecule HPK1 inhibitor, was specifically designed to address the selectivity challenge against other closely related MAP4K family members.<sup>33</sup>

Consistent with the genetic *hpk1* knockout studies, pharmacological inhibition of HPK1 with NDI-101150 has shown broad immunomodulatory activity in preclinical systems that are associated with primary or acquired resistance to CPI therapy.<sup>34</sup> NDI-101150 reinvigorated exhausted human T cells and restored effector function in the presence of suppressive mediators such as transforming growth factor  $\beta$ , adenosine, and PGE2, where checkpoint inhibition is not expected to and, in fact, did not have any effect. In addition to its effect on T cells, NDI-101150 enhanced B cell and DC activity, increasing cytokine secretion and co-stimulatory receptor expression on bone-marrow-derived DCs, respectively. *In vivo*, treatment with NDI-101150 resulted in robust tumor growth inhibition and generation of long-term immune memory in the EMT-6 syngeneic mouse model, with tumors showing increased infiltration of cytotoxic CD8<sup>+</sup> T cells, CD19<sup>+</sup> B cells, and DCs. NDI-101150 also showed efficacy in syngeneic mouse tumors that are less sensitive to anti-PD1.

To evaluate the clinical activity of NDI-101150, we conducted a human phase 1/2 trial in patients with advanced solid tumors

that were refractory to standard-of-care (SOC) therapies, including those who had progressed on prior CPIs. The initial dose escalation assessed the safety and tolerability of NDI-101150, both as a monotherapy or in combination with SOC pembrolizumab. Once a monotherapy maximum tolerated dose (MTD) was determined, tumor-specific expansion cohorts were initiated in renal cell carcinoma (RCC), non-small cell lung cancer (NSCLC), and gastric/gastro-esophageal junction (G/GEJ) cancers. Here, we report final outcomes for safety, efficacy, PK, PD, and exploratory translational studies.

## RESULTS

### Patients

Between 03 November 2021 and 11 November 2024, a total of 106 patients with advanced solid tumors were enrolled in the study, including 94 receiving NDI-101150 monotherapy and 12 patients receiving NDI-101150 and pembrolizumab as a combination therapy (Figure 1). Overall, the most common tumor types were RCC ( $n = 38$ ; 36%), NSCLC ( $n = 17$ ; 16%), and G/GEJ cancer ( $n = 12$ ; 11%). There were 39 patients (37%) with other tumor types, including pancreatic, colorectal, endometrial, melanoma, ovarian, anal, tonsil, uterine, chondrosarcoma, and soft tissue sarcoma. Fifty seven percent of the participants were male with a median age of 66 years (range: 21–90 years). Median number of prior treatments was 3 (range: 0–10), and 69 patients (63%) had received prior immunotherapy (Tables 1, S1, S2, and S3; Data S1).

Of the 106 patients, 53 patients were enrolled in the dose escalation phase and 53 were enrolled in the dose expansion phase. In the dose escalation phase, patients with any type of advanced solid tumors were treated with one of the five doses of NDI-101150 monotherapy (50, 100, 140, 150, and 200 mg, once daily oral dosing) or one of the two doses of NDI-101150 (50 or 100 mg, once daily oral dosing) in combination with 200 mg of pembrolizumab (dosed intravenously every 3 weeks). In the dose expansion phase, patients with RCC received either 100 or 150 mg of NDI-101150 monotherapy, and patients with NSCLC or G/GEJ cancer received 100 mg of NDI-101150 monotherapy. NDI-101150 and pembrolizumab combination therapy was not tested in the dose expansion phase.

### Safety

The safety analysis set comprised all 106 patients. A summary of the treatment-related adverse events (TRAEs) is listed in Table 2, with a more detailed summary stratified by dose and treatment condition (monotherapy vs. combination) listed in Tables S4, S5, S6, S7, and S8. In the monotherapy cohort, 79% of patients across all doses experienced any grade TRAE, with the most common TRAEs being nausea (43%), diarrhea (35%), vomiting (29%), fatigue (29%), and anemia (11%). Grade  $\geq 3$  TRAEs occurred in 13 (14%) patients, of which there was one incidence (1%) of grade 4 TRAE (aplastic anemia). The most common grade  $\geq 3$  TRAEs were fatigue (2%), dyspnea (2%), lymphocyte count decreased (1%), diarrhea (1%), colitis (1%), anemia (1%), and proteinuria (1%). The incidence of grade  $\geq 3$  TRAEs was lower in the 50–150 mg cohorts (11%) compared with the 200 mg cohort (44%). Immune-related AEs (irAEs) in the

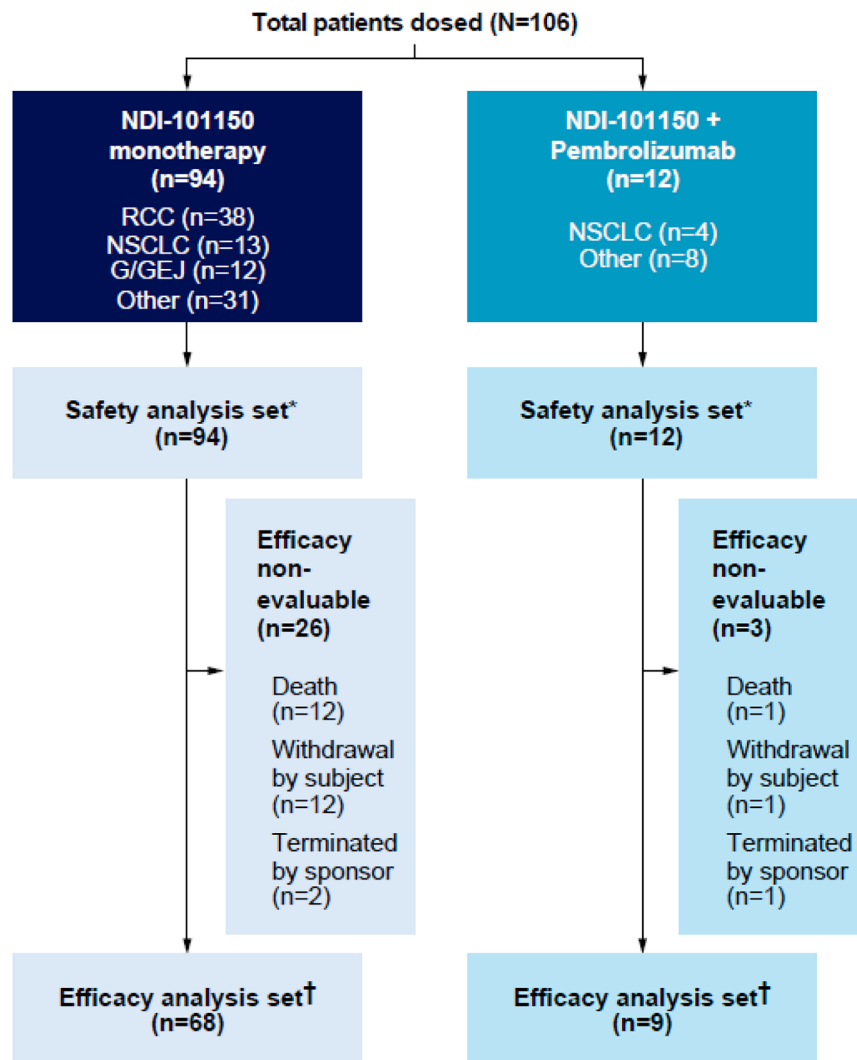


**Figure 1. Consort diagram**

A flow diagram detailing patients enrolled in the study. \*Includes patients who receive any amount of IMP (NDI-101150) monotherapy or in combination with pembrolizumab. The Safety Analysis Set is the primary analysis set for all safety endpoints, excluding DLT evaluation. †Includes all patients with measurable disease at baseline who receive assigned IMP and have at least one post-baseline response assessment.

disorder, and immune-mediated arthritis). There were no irAEs reported in the 100 mg combination arm. Combina-bility was demonstrated for both the 50 and 100 mg dose of NDI-101150 with pembrolizumab, and an MTD for the combination therapy was not reached.

### Efficacy

The efficacy analysis set included 77 response-evaluable patients (68 in the monotherapy arm and nine in the combi-nation arm with pembrolizumab), all of whom had measurable disease at base-line and at least one post-baseline assessment after receiving a minimum of one dose of NDI-101150. Among these, patients with RCC ( $n = 32$ ) demon-strated the best overall response to NDI-101150 monotherapy (Table 3; Figure 2A). Within RCC, three of 22 patients achieved objective responses (13.6%, 95% confidence interval [CI]: 2.9%–34.9%) in clear cell RCC (ccRCC), the most common RCC subtype; one pa-tient in the 50 mg cohort experienced a confirmed complete response (CR), while

monotherapy arm (occurring in  $\geq 3$  patients) included skin and subcutaneous disorders (5%), immune-mediated dermatitis (3%), gastrointestinal disorders (3%) and immune-mediated lung disease (3%) (Table S9). Three patients experienced dose-limiting toxicities (DLTs) at 200 mg including acute kidney injury, pneumonitis, and fatigue (all grade 3), whereas no patients experienced DLTs in the 50–150 mg cohorts. Hence, following a standard 3 + 3 dose escalation design, 200 mg was declared as a non-tolerated dose and 150 mg was identified to be the MTD.

In patients receiving NDI-101150 and SOC pembrolizumab as a combination therapy, the incidence, class, and severity of TRAEs were comparable to NDI-101150 monotherapy. In the combination arm ( $n = 12$ ), the most frequently reported any-grade TRAEs were diarrhea (33%), nausea (33%), vomiting (25%), constipation (17%), and fatigue (17%). Grade  $\geq 3$  TRAEs were constipation and elevated AST, both occurring in 1 (8%) patient each. There were two subjects at the 50 mg dose level combination arm that experienced irAEs (immune system disorder, cytokine release syndrome, musculoskeletal

two patients in the 100 mg cohort achieved confirmed partial responses (PRs; Figure 2B). These responders had markedly different responses to prior CPI. The patient with a CR had previously received two lines of therapy in the advanced setting, including a tyrosine kinase inhibitor (TKI, pazopanib), followed by a CPI (nivolumab), with prolonged responses of approximately 22 and 45 months, respectively. The patient progressed on nivolumab as manifested by a new lung lesion and was subsequently treated with 50 mg NDI-101150 47 days following the last dose of nivolumab. This resulted in a PR at first disease assessment by computed tomography (CT) scan at 8 weeks post 1<sup>st</sup> dose and was completely resolved at the second disease assessment after an additional 8 weeks, with the patient continuing to be on NDI-101150 treatment at 50 mg for 8.5 months (Figure 2C). In contrast, one patient with a PR, treated with 100 mg NDI-101150, was refractory to prior CPI therapy (nivolumab). This patient had four reported prior lines of therapy and responded well to two separate regimens of TKIs—first to cabozantinib for 32 months and then to tivozanib

**Table 1. Baseline characteristics of patients receiving NDI-101150 monotherapy and NDI-101150 + pembrolizumab combination therapy**

		Monotherapy (N = 94)	Combination therapy (N = 12)	Overall (N = 106)
Age, median (min–max)		66 (21–90)	66 (49–83)	66 (21–90)
Gender, n (%)	Male	53 (56.4)	7 (58.3)	60 (56.6)
	Female	41 (43.6)	5 (41.7)	46 (43.4)
Tumor type, n (%)	RCC	38 (40.4)	0	38 (35.8)
	ccRCC	29 (30.8)	0	29 (27.3)
	non-ccRCC	9 (9.5)	0	9 (8.4)
	NSCLC	13 (13.8)	4 (33.3)	17 (16.0)
	G/GEJ	12 (12.8)	0	12 (11.3)
	Other	31 (33.0)	8 (66.7)	39 (36.8)
ECOG PS score	0	31 (33.0)	5 (41.7)	36 (34.0)
	1	63 (67.0)	7 (58.3)	70 (66.0)
Prior lines of therapy, median (min–max)		3 (0–10)	3 (1–8)	3 (0–10)

ECOG PS, Eastern Cooperative Oncology Group performance status; ccRCC, clear cell renal cell carcinoma; G/GEJ, gastric and gastroesophageal junction; nccRCC, non-clear cell renal cell carcinoma; NSCLC, non-small cell lung cancer; PS, performance status; RCC, renal cell carcinoma; TRAE, treatment-related adverse event.

Note: the risk status was determined in those patients enrolled in the dose expansion phase of the study.

for 14 months—while an interspersed CPI therapy with nivolumab was not effective, as disease progression was observed in under 2 months (Figure 2D). The second patient with a PR had undergone six prior lines of therapy, including a TKI/CPI combination, with better outcomes on combination therapy (on therapy for 2+ years) than on CPI monotherapy (on nivolumab for ~2.5 months; Figure 2E). Based on these case studies,

NDI-101150 treatment results in anti-tumor activity with substantial clinical benefit to ccRCC patients who are heavily pre-treated (up to six prior lines) and refractory to or progressed on prior CPI. In addition to the patients with either a CR or PR, three ccRCC patients had durable SD for approximately 8, 11, and 25 months, respectively. Overall, six patients (27.3%, 95% CI: 10.7%–50.2%) with ccRCC derived clinical benefit (CR + PR +

**Table 2. Most common any grade and ≥ grade 3 TRAEs in patients receiving NDI-101150 monotherapy or NDI-101150 + pembrolizumab combination therapy**

Preferred term, n Patients (%)	Monotherapy (n = 94)				Combination (n = 12)	
	50-150 mg QD (n = 85)		200 mg QD (n = 9)		50 or 100mg NDI-101150 + SoC Pembro	
	Any grade	≥ Grade 3	Any grade	≥ Grade 3	Any grade	≥ Grade 3
Patients at least one TRAE	66 (77.6)	9 (10.6)	8 (88.9)	4 (44.4)	11 (91.7)	2 (16.7)
95% CI	67.3%, 86.0%	5.0%, 19.2%	51.8%, 99.7%	13.7%, 78.8%	61.5%, 99.8%	2.1%, 48.4%
Nausea	37 (43.5)	0	3 (33.3)	0	4 (33.3)	0
Diarrhea	27 (31.8)	0	6 (66.7)	1 (11.1)	4 (33.3)	0
Fatigue	24 (28.2)	1 (1.2)	3 (33.3)	1 (11.1)	2 (16.7)	0
Vomiting	22 (25.9)	0	5 (55.6)	0	3 (25.0)	0
Anemia	9 (10.6)	1 (1.2)	1 (11.1)	0	0	0
Blood creatinine increased	7 (8.2)	0	0	0	0	0
Decreased appetite	5 (5.9)	0	0	0	0	0
Pruritus	5 (5.9)	0	1 (11.1)	0	0	0
Platelet count decreased	4 (4.7)	1 (1.2)	1 (11.1)	0	0	0
Constipation	3 (3.5)	0	1 (11.1)	0	2 (16.7)	1 (8.3)
Dyspnea	3 (3.5)	2 (2.4)	1 (11.1)	0	0	0
Immune-mediated dermatitis	3 (3.5)	0	0	0	0	0
Proteinuria	3 (3.5)	1 (1.2)	0	0	0	0

CI, confidence interval (Clopper-Pearson method); TRAE, treatment-related adverse event; QD, once daily dosing.

Note: patients reporting more than one event are counted only once for each preferred term.

Table 2 lists the most common TRAE experienced in three or more patients in the 50–150 mg monotherapy group.

**Table 3. Summary of responses in patients receiving NDI-101150 monotherapy**

BOR, n (%)	RCC			NSCLC (n = 8)	G/GEJ (n = 9)	Other* (n = 19)	Total (n = 68)
	ccRCC (n = 22)	nccRCC (n = 10)	All RCC (n = 32)				
CR	1 (4.5)	0	1 (3.1)	0	0	0	1 (1.5)
PR	2 (9.1)	0	2 (6.3)	0	0	0	2 (2.9)
SD	9 (40.9)	3 (30.0)	12 (37.5)	2 (25.0)	2 (22.2)	2 (10.5)	18 (26.5)
PD	10 (45.5)	7 (70.0)	17 (53.1)	6 (75.0)	7 (77.8)	16 (84.2)	46 (67.6)
NE	0	0	0	0	0	1 (1.5)**	1 (1.5)**
ORR	3 (13.6)	0	3 (9.4)	0	0	0	3 (4.4)
ORR 95% CI	2.9%,34.9%	0.0%,30.8%	2.0%,25.0%	0.0%,36.9%	0.0%,33.6%	0.0%,17.6%	0.9%,12.4%
CBR	6 (27.3)	0	6 (18.8)	0	0	2 (10.5)	8 (11.8)
CBR 95% CI	10.7%,50.2%	0.0%,30.8%	7.2%,36.4%	0.0%,36.9%	0.0%,33.6%	1.3%,33.1%	5.2%,21.9%
DCR	12 (54.5)	3 (30.0)	15 (46.9)	2 (25.0)	2 (22.2)	2 (10.5)	21 (30.9)
DCR 95%CI	35.2%, 75.6%	6.7%, 65.2%	29.1%, 65.3%	3.2%, 65.1%	2.8, 60.0%	1.3%, 33.1%	20.2%, 43.3%

Note: two-sided 95% confidence interval calculated using the exact Clopper-Pearson method for binomial proportions.

\*Other tumor types include pancreatic, colorectal, endometrial, melanoma, ovarian, anal cancer, chondrosarcoma, soft tissue sarcoma, tonsil, and uterine. One of the 19 patients in the “other” tumor category was evaluable for response; however, the overall disease assessment classified the patient as non-evaluable due to one of the target lesions being unmeasurable.

\*\*One of the 19 patients in the “other tumor” category was evaluable for response; however, the overall disease assessment classified the patient as non-evaluable.

Abbreviations: ccRCC, clear cell renal cell carcinoma; CBR, clinical benefit rate; CR, complete response; CI, confidence interval; DCR, disease control rate; dSD, durable stable disease; ORR, objective response rate; nccRCC, non-clear cell renal cell carcinoma; NE, non-evaluable; PD, progressive disease; PR, partial response; GEJ, gastric and esophageal junction; RCC, renal cell carcinoma; NSCLC, non-small cell lung cancer; SD, stable disease; PD, progressive disease. dSD, SD for 6 months or longer; ORR, CR + PR/total; CBR, CR + PR + dSD/total; DCR, CR + PR + SD/total.

SD  $\geq$  6 months) and 12 (54.5%, 95% CI: 32.25%–75.6%) experienced disease control (CR + PR + SD of any duration) with NDI-101150 monotherapy. Clinical benefit and disease control were observed across multiple dose levels, indicating that the dose range of 50–150 mg was efficacious.

Preliminary disease control with NDI-101150 monotherapy was also observed in other tumor types, including pancreatic and endometrial cancers. One pancreatic cancer patient treated with 200 mg achieved SD for approximately 14 months, while an endometrial cancer patient treated with 150 mg maintained SD for 7 months (Figure 2B). No additional objective responses were observed within the non-ccRCC monotherapy or combination arms. Of note, no RCC patients were enrolled in the combination cohort.

### Pharmacokinetics

All 106 subjects were evaluable for PK analysis, including six patients specifically enrolled to assess the effect of food on PK (food effect). Following oral administration of NDI-101150 (50, 100, 140, 150, and 200 mg as monotherapy; 50 and 100 mg in combination with pembrolizumab), time to maximum concentration ( $T_{max}$ ) ranged from 1 to 8 h, with comparable exposures observed between monotherapy and combination cohorts. NDI-101150 mean half-life ranged from 6 to 10 h across cohorts. Dose proportionality for both maximum observed plasma concentration ( $C_{max}$ ) and area under the plasma concentration-time curve from time zero to 24 h post-dose ( $AUC_{0-24h}$ ) was observed between 50 and 150 mg on cycle 1 day 1 (C1D1), cycle 1 day 15 (C1D15), and cycle 2 day 1 (C2D1), although values at 150 and 200 mg overlapped within standard deviations. Meaningful accumulation ( $\geq$ 2-fold) in  $C_{max}$  and  $AUC_{0-24h}$  occurred at

doses  $\leq$ 150 mg (monotherapy and combination) between C1D1 and C1D15/C2D1, while minimal accumulation at 200 mg was likely attributable to increased vomiting in both frequency and duration. In a pilot food-effect cohort at the 150 mg dose, high-fat meals resulted in delayed absorption and 45% and 22% decreases in  $C_{max}$  and  $AUC_{0-24h}$ , respectively, compared to the fasted state; however, no exposure differences were anticipated in fed states. Plasma concentration profiles over time for fasted patients and detailed PK parameters for all patients (fed and fasted) are provided in Figure 3A and Tables S10, S11, and S12. Together, these results demonstrate that NDI-101150 exhibits predictable, dose-proportional PK between 50 and 150 mg, with similar exposures when dosed as monotherapy or in combination with pembrolizumab. In addition, initial data suggest a minimal clinically meaningful food effect.

### Pharmacodynamic studies

To determine the level of HPK1 inhibition that NDI-101150 achieved in patients, a whole blood assay was developed to assess phosphorylated SLP76 following *ex vivo* stimulation (anti-CD3/anti-CD28). Upon T cell receptor activation, SLP76 is directly phosphorylated by HPK1, leading to its degradation and negative regulation of the T cell activation cascade. Therefore, the reduction in pSLP76 levels serves as a measure of HPK1 inhibition mediated by NDI-101150 treatment. Preclinical dose fractionation studies in a CT-26 syngeneic tumor model indicated that maintaining at least 50% reduction of pSLP76 for 14–18 h was required to observe anti-tumor activity (Figure S1).<sup>34</sup> Phospho-SLP76 data were available for 65 of 106 patients treated on-study across all monotherapy and combination cohorts. The reasons for analysis failure in the 41

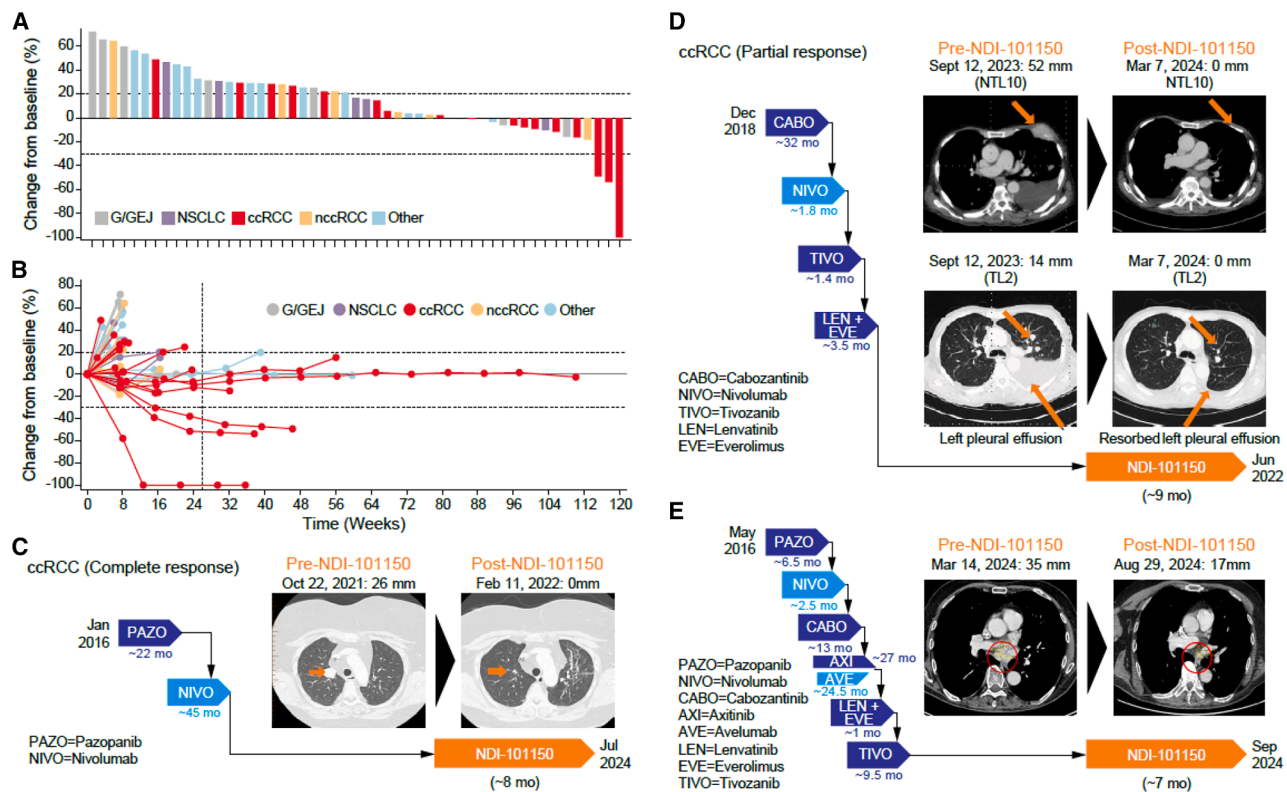


**Figure 2. Best overall response in patients receiving NDI-101150 monotherapy, with scans showing changes in target lesion pre- and post-treatment with NDI-101150 monotherapy**

ccRCC, clear cell carcinoma; G/GEJ, gastric and esophageal junction; nccRCC, non-clear cell carcinoma; NSCLC, non-small cell lung cancer; RCC, renal cell carcinoma. Other tumor types included pancreatic, colorectal, endometrial, melanoma, ovarian, rectal cancer, chondrosarcoma, soft tissue sarcoma, tonsil cancer, and uterine cancer.

(A) Waterfall plot shows the best percent change in sums of target lesion size compared to baseline for individual patients ( $n = 51$ ). Indications shown include G/GEJ, NSCLC, ccRCC, and RCC not diagnosed as clear cell (nccRCC).

(B) Spider plot of best overall response in patients ( $n = 51$ ) who received NDI-101150 monotherapy evaluated based on RECIST v.1.1. Each line represents one patient, the indications shown include G/GEJ, NSCLC, ccRCC, and RCC not diagnosed as clear cell (nccRCC). The horizontal dotted lines at +20% represent cutoffs for progressive disease and at -30% represent cutoffs for partial response. The vertical dotted line represents the six-month cutoff and is representative of those patients achieving durable SD.

(C) Vignette of a patient with ccRCC who had a complete response after NDI-101150 monotherapy.

(D) Vignette of a patient with ccRCC who had a partial response after NDI-101150 monotherapy.

(E) Vignette of a patient with ccRCC who had a partial response after NDI-101150 monotherapy.

patients with insufficient data included failure of T cells to respond to *ex vivo* anti-CD3/anti-CD28 stimulation, technical quality control failures, and samples either not being received or received out of the stability window. On cycle 1 day 1, a clear PK/PD relationship was observed (Figure 3B), with nonlinear regression analysis identifying a clinical pSLP76 half maximal inhibitory concentration ( $IC_{50}$ ) of 64 ng/mL total drug exposure. By day 15, steady state plasma concentrations at all doses of NDI-101150 exceeded the pSLP76  $IC_{50}$  for a period consistent with pre-clinical dose fractionation studies. Additionally, longitudinal analysis of pSLP76 showed that by day 8 all doses achieved >50% inhibition (Figure S2). Importantly, no meaningful differences were observed in pSLP76 inhibition between monotherapy and pembrolizumab combination samples, indicating a consistent effect of NDI-101150 across both treatment settings.

To determine whether NDI-101150-mediated HPK1 inhibition altered pSLP76 levels in the TME, paired pre- and on-treatment

tumor biopsies from 14 patients were analyzed using a two-plex (CD3 and pSLP76) immunofluorescence assay. After approximately 28 days of therapy, there was a 73% reduction in the mean percentage of CD3+pSLP76+ cells compared to baseline (Wilcoxon signed-rank test, single-hypothesis  $p = 0.025$ ), with 71% (10/14) of patients exhibiting a decreased percentage of CD3+pSLP76+ cells following NDI-101150 treatment (Figure 3C).

### Translational analyses

A multiplex immunophenotyping assay was developed and performed on 12 paired pre-dose and on-treatment tumor biopsies to evaluate the effect of NDI-101150 on immune cells in the tumor after 28 days of treatment. In 10 of 12 patients, an increase in the percentage of activated CD8+ T cells was observed on treatment. Overall, a 2.5 $\times$  median increase in CD8+granzymeB+ (baseline median = 3.7%, on-treatment median = 8.7%) and

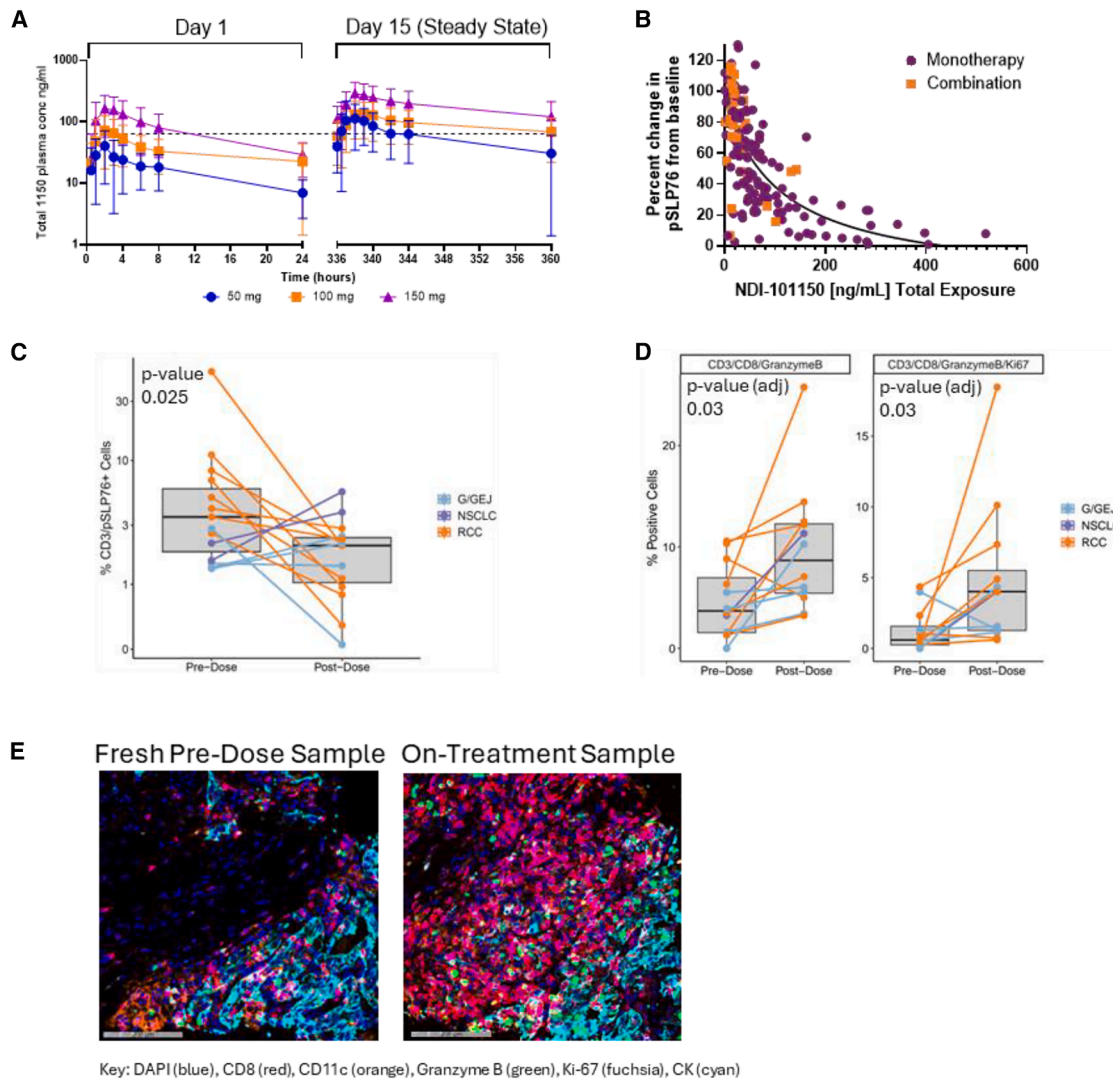


**Figure 3. Pharmacokinetic, pharmacodynamic, and translational outcomes**

Pharmacokinetic, pharmacodynamic, and translational results from advanced solid tumor patients treated with NDI-101150 are shown.

(A) NDI-101150 total plasma concentrations, expressed as mean  $\pm$  SD, had a near dose-proportional increase on day 1, with drug accumulation observed at steady state (day 15) sufficient to cover the pSLP76 whole blood clinical  $IC_{50}$  (represented by the dashed line). Doses represented include 50 mg (blue line; 0–24 h,  $n = 8$ ; 336–360 h,  $n = 3$ ), 100 mg (orange line; 0–24 h,  $n = 43$ ; 336–360 h,  $n = 30$ ), and 150 mg (purple line; 0–24 h  $n = 27$ ; 336–360 h,  $n = 22$ ).

(B) A relationship between total NDI-101150 exposure and inhibition of the pSLP76 at C1D1 was established, including a clinical  $IC_{50}$  of 67 ng/mL (total concentration). Data from the combination ( $n = 28$  points, including from available time points with both PK and PD data from 10 patients) cohorts are included, with no differences observed when compared to monotherapy ( $n = 141$  points, including from available time points with both PK and PD data from 55 patients).

(C) Tissue pSLP76 data from 13 patients was collected utilizing a 2-Plex (CD3, pSLP76) immunofluorescence assay; results from tissue samples collected following 28 ( $\pm 7$  days) of NDI-101150 treatment show a clear reduction in percent CD3+pSLP76 cells compared to tissue samples collected pre-NDI-101150 treatment (Wilcoxon signed-rank test, single-hypothesis  $p = 0.025$ ).

(D) Quantitative analysis of whole slide images from the individual patients ( $n = 11$ ) with paired pre-dose and on-treatment biopsies show an increased number of CD8 T cells that are activated either through the co-expression of granzyme B or both granzyme B and Ki-67 in the on-treatment sample (Wilcoxon signed-rank test,  $p = 0.004$ , FDR-adjusted  $p = 0.03$ ).

(E) 12-Plex representative images from a clear cell RCC patient at baseline and following 28 days of NDI-101150 treatment at 100 mg QD are shown, demonstrating an increase in the CD8 cells that are activated through the increased expression of granzyme B and increase of dendritic cells represented by CD11c. Scale bar represents 200  $\mu$ m. See also [Figures S1, S2, S3, S4, and S5](#); [Tables S10, S11, S12, S13, and S14](#).

approximately 6.5 $\times$  median increase in CD8+granzymeB+Ki67+ (baseline median = 0.6%, on-treatment median = 4.01%) cells were observed, with both increases being statistically significant (Wilcoxon signed-rank test,  $p < 0.01$ ; [Figure 3D](#)). Of the 12

pre-dose biopsies, eight were considered fresh (biopsy taken within 28 days prior to NDI-101150 treatment) while four were archival (range 1–5 years prior to NDI-101150 treatment). There were no observed differences in the percentage of cells detected

between the fresh and archive pre-dose biopsies (Table S13), demonstrating that the archival samples analyzed were representative of the pre-dose TME. In Figure 3E, representative baseline and on-treatment images from a patient with ccRCC who underwent fresh biopsies of a rib metastasis at baseline and on day 28 are shown. These images show a marked increase in CD8<sup>+</sup> cells post-treatment, with many of the cells co-expressing activation markers granzyme B and/or Ki-67. Within the images, cytokeratin staining clearly delineates tumor borders, demonstrating that the increase in CD8<sup>+</sup> T cells following NDI-101150 treatment is observed in both tumor and peri-tumor regions. These results align with broader preclinical data showing robust immune cell recruitment and activation within the TME following HPK1 inhibition. Evaluation of PD-1 and LAG3 on CD3<sup>+</sup>CD8<sup>+</sup> cells showed only minimal increases, indicating that NDI-101150 did not induce phenotypic exhaustion in tumor-infiltrating CD8 T cells within the first 28 days of treatment (Figure S3). Similarly, the number of T regulatory cells in the on-treatment samples were also only marginally elevated compared to the baseline samples (Table S14).

To broaden and corroborate the immunophenotyping findings, we performed digital spatial profiling of tissue biopsies using the whole transcriptome GeoMx assay. To refine our analysis, tissue samples were annotated into tumor and non-tumor regions by pathologist-reviewed H&E-stained slides. By comparing gene expressions from regions of interest in a set of 10 paired pre and on-treatment biopsy samples across indications (ccRCC  $n = 8$ , G/GEJ  $n = 1$ , and NSCLC  $n = 1$ ), we observed significant enrichment of multiple immune-related gene sets upregulated in the tumor compartment on treatment. Many of these gene sets, such as those reflecting cytotoxic CD8 T cell activation (e.g., *PRF1*, *GZMB*, *FASLG*, and *CXCR6*), corroborate results from the 12-plex assay that show an increase in T cell activation markers (granzyme B+ and Ki67+) following NDI-101150 treatment. In addition, we detected increased expression of genes related to activation of the interferon response (e.g., *STAT1*, *IRF1*, *GBP4*, and *ISG15*) and presence of myeloid dendritic cells (e.g., *D86*, *XCR1*, *CD33*, and *SLAMF8*), extending the 12-plex findings and consistent with the proposed mechanism of HPK1 inhibition from pre-clinical studies<sup>34</sup> (signatures,  $p < 0.05$ , Wilcoxon signed-rank test; Figure S4).

## DISCUSSION

Here, we report that NDI-101150, a potent highly selective HPK1 inhibitor, exerts immunomodulatory effects through a mechanism of action that broadly activates B cells, DCs, and T cells, leading to robust monotherapy anti-cancer activity. Notably, this effect persists in tumor settings that have become resistant or are refractory to checkpoint inhibition, including in ccRCC patients who had progressed on multiple previous therapies. Among 22 response evaluable patients with ccRCC, three patients (13.6%) achieved an objective response, including one CR and two PRs, and three additional patients achieved durable SD, lasting approximately 8, 11, and 25 months, respectively, resulting in a clinical benefit rate (CBR) of 27.3% and a disease control rate (DCR) of 54.5%. There were limited sample sizes in the expansion cohorts for NSCLC and G/GEJ, constraining a

true efficacy analysis (particularly given the biological heterogeneity of these tumors). Moving forward, biomarker discovery to identify patients with other tumor types that may benefit from HPK1 inhibition should be prioritized.

NDI-101150 was well tolerated both as monotherapy and in combination with the anti-PD-1 antibody pembrolizumab in patients with advanced solid tumors. The MTD for monotherapy was determined to be 150 mg once daily, while combinability with pembrolizumab was demonstrated to be 100 mg of NDI-101150. An MTD in the combination setting was not established. In the monotherapy cohorts up to 150 mg, grade 3 or higher TRAEs were uncommon (11% of patients, 50–150 mg doses). In comparison, other reported HPK1 inhibitors tested in the clinic have not been able to demonstrate single agent anti-cancer activity coupled with a favorable safety profile like NDI-101150. Previously, CFI-40211, an HPK1 inhibitor, administered alone or in combination with pembrolizumab reported DCRs of 18% and 29%, respectively, but was associated with high-grade TRAEs in over half of the patients,<sup>35</sup> resulting in a potentially unfavorable risk/benefit ratio. BGB-1502, another HPK1 inhibitor, was evaluated as a monotherapy or in combination with the anti-PD-1 inhibitor tislelizumab in patients with CPI-refractory advanced solid tumors. While the monotherapy arm showed a manageable safety profile (grade  $\geq 3$  TRAE rate of 12%), no objective responses were observed, and target engagement was limited.<sup>36</sup> One potential explanation for greater activity of NDI-101150 is its selectivity: NDI-101150 is 377-fold more selective for HPK1 relative to GLK, a closely related MAP4K family kinase that promotes immune cell signaling, thus leading to effective immune suppression. HPK1 inhibitors with weaker selectivity across MAP4K kinases such as GLK may lose efficacy because the effect is counteracted by GLK-dependent signaling dampening the immune response in the absence of exquisite selectivity.

Clinical PK, PD, and translational analyses further supported the monotherapy activity observed with NDI-101150. Dose-proportional increases in plasma exposure were observed between 50 and 150 mgs on day 1, with steady-state exposures in all dose cohorts exceeding the IC<sub>50</sub> for the PD biomarker pSLP76, which was shown previously to be required for efficacy in pre-clinical dose fractionation studies. This was a key finding since we had observed objective responses at our lowest starting dose of 50 mg in our study. Through our translation studies, we confirmed the proposed mechanism of action described in pre-clinical models by demonstrating an increased immune cell infiltration and gene expression changes consistent with immune modulation post-NDI-101150 treatment<sup>34</sup> (though we acknowledge the limitation of a limited sample size for translational analysis, which can introduce selection bias and potentially limit generalizability). Complementary to the 12-plex findings, digital spatial profiling confirmed upregulation of immune-activating gene sets, including those involved in the interferon response and CD8<sup>+</sup> T cell activation, as well as genes associated with the presence of dendritic cells. Taken together, the monotherapy responses observed in heavily pre-treated patients, especially those who had progressed on prior CPI, are consistent with the hypothesis and potential of NDI-101150 to be effective in these hard-to-treat patient populations. Additionally, the

responses seen in our study occurred in patients who had varying responses to prior CPI, demonstrating the potential of HPK1 inhibition through NDI-101150 to provide benefit to patients who have progressed on a range of prior therapies and combinations that are consistent with the current treatment landscape in ccRCC.

To further develop NDI-101150 and determine how it could fit in the current treatment landscape in RCC and other indications of unmet need, it is important to contextualize our results within the sequence of current regimens and recently published clinical studies. The TiNivo-2<sup>37</sup> and CONTACT-03<sup>38</sup> trials reported on the efficacy of CPI rechallenge (in combination with a TKI) in advanced RCC patients that had progressed on prior CPI therapy. Both studies demonstrated no clinical benefit from adding existing CPIs to TKIs as a combination in this post-CPI refractory setting, highlighting the challenge of immunotherapies in the post-CPI setting. In contrast, NDI-101150, which exerts a broad-ranging mechanism of action by modulating both adaptive and innate immunity through HPK1 inhibition in B cells, DCs, and T cells, has shown promising monotherapy activity specifically in patients who were refractory to or had progressed on prior CPI therapy. These early findings support the hypothesis that CPI-refractory RCC tumors that otherwise do not typically respond to a rechallenge with current CPIs with a similar mechanism of action may be sensitive to HPK1 inhibitors and could address the high unmet medical need for additional effective treatments for RCC patients who have exhausted prior therapies.

Recently, belzutifan, an agent with a mechanism of action targeting hypoxia-inducible factor-2 alpha was approved for treatment in adult patients with von Hippel-Lindau-disease-associated RCC who do not require immediate surgery as well as use in pretreated advanced clear cell RCC after progression on prior CPI and vascular endothelial growth factor (VEGF)-targeted therapy. Moreover, two belzutifan combination trials additionally reported positive outcomes, demonstrating improved progression-free survival (PFS) and objective response rate (ORR) by combining with lenvatinib, a multiple TKI, in RCC patients who had progressed on prior CPI therapies as well as in combination with pembrolizumab in the adjuvant setting, showing superior disease-free survival (DFS) compared to SOC pembrolizumab alone,<sup>39,40</sup> thus positioning belzutifan potentially into earlier lines of therapy. Given these positive data readouts with complementary mechanism of actions especially in patients who were previously refractory or had progressed on prior CPIs in addition to positioning in the adjuvant setting, an immunomodulatory mechanism like a HPK1 inhibitor similarly offers potential for combinations with multiple agents given their complementary mechanisms (HIF2alpha, TKI or anti-PD1) for patients progressing on prior CPI and TKI regimens, leading to potentially broader and deeper clinical response.

Of particular interest is to also examine the effects of an HPK1 inhibitor in combination with a CPI and/or belzutifan as frontline exposure. This needs to take the evolving treatment landscape in RCC in context. In the adjuvant setting for intermediate-high or high-risk RCC, the new SOC could possibly include belzutifan in combination with pembrolizumab. Additionally, first-line

RCC treatments currently include an ipilimumab-nivolumab or CPI-TKI combination. In view of the TiNivo-2 and CONTACT-03 studies, it will be interesting to see whether CPI-CPI or CPI-TKI first-line treatment paradigm will remain SOC with the current use of a pembrolizumab-based treatment regimen in the adjuvant setting. This further provides a rationale for an immunomodulator like NDI-101150 in combination with either a CPI, TKI, or HIF2alpha inhibitor to be assessed as a valuable treatment option for earlier lines in the future. One limitation of our human phase 1/2 study is the small and heterogeneous patient population with a broad range of prior therapies across diverse tumor types. It will be interesting to further examine efficacy and safety in a more homogenous patient population to validate and contextualize our early findings, which requires larger controlled studies.

In conclusion, this human study demonstrated that NDI-101150, a potent and selective HPK1 inhibitor, delivers a manageable safety profile with impressive single-agent activity in heavily pretreated patients with advanced solid tumors, particularly in those with ccRCC who have stopped responding to SOC treatments, including CPIs. The observed objective responses, durable disease control, and immune activation of the TME provide clinical validation for this immunomodulatory mechanism of action in a challenging patient population. To our knowledge, the observation of robust single-agent activity with this immunotherapy follows a long period of rather disappointing results of other check point inhibitors or immunomodulatory agents.<sup>41,42</sup> Collectively these findings support the continued clinical development of NDI-101150 across both early and later lines of therapy and underscore the need for larger, randomized studies to confirm its efficacy and define its role within the evolving treatment landscape for advanced solid tumors.

### Limitations of the study

The single-arm phase 1/2 study is limited by its open-label design and lacks a randomized comparator, restricting definitive assessment of NDI-101150 benefit. In addition, data from this study demonstrate that NDI-101150 has a favorable safety profile as monotherapy or in combination with pembrolizumab, monotherapy anti-tumor activity in ccRCC, and on-target activation of the tumor immune environment; further studies in a larger and less heterogeneous patient population will be needed to confirm and expand these findings in both mono and combination therapies.

### RESOURCE AVAILABILITY

#### Lead contact

Further information and requests for resources should be directed to and will be fulfilled by the lead contact, David Braun ([david.braun@yale.edu](mailto:david.braun@yale.edu)).

#### Materials availability

This study did not generate new unique reagents.

#### Data and code availability

- The datasets generated and analyzed during this study are not deposited in a public repository due to the sponsor's policy on maintaining patient privacy. Data access supporting the findings of this study are available upon request. Qualified researchers may obtain access to de-identified data by contacting the [lead contact](#), David Braun ([david.braun@yale.edu](mailto:david.braun@yale.edu)).

[braun@yale.edu](mailto:braun@yale.edu)). Requesters will be asked to describe the objectives of their proposed research and enter into a data sharing agreement with the study sponsor. Data access will be granted for research and non-commercial use only.

- This paper does not report original code.
- Any additional information required to reanalyze the data reported in this paper is available from the [lead contact](#) David Braun ([david.braun@yale.edu](mailto:david.braun@yale.edu)) upon request.

## ACKNOWLEDGMENTS

This study was funded by Nimbus Therapeutics (Nimbus Discovery Inc. on behalf of Nimbus Saturn Inc.). We thank Todd Bowser for support in preparing the manuscript; Peter Tummino, Christine Loh, and Robert Svensson for additional review of the manuscript; Tom Peppard for statistical support; Nathalie Rioux for clinical pharmacology support; Erica Allen for medical writing support; Ji Chen for QC and programming support; and Eric Smith for graphics support. We also thank CellCarta, Ultivue, and Canopy Bioscience for assistance in conducting the experiments.

## AUTHOR CONTRIBUTIONS

The manuscript was prepared and edited by D.A.B., S.R.D., S.N., P.K., and A.S. T.K.C. provided feedback and review of the original and revised versions of the figures and manuscripts. All authors reviewed and agreed on the final version of the manuscript. P.K., S.N., and A.S. oversaw the statistical analyses and had unrestricted access to all data.

## DECLARATION OF INTERESTS

D.A.B. reports stock and other ownership interests in CurIOS Therapeutics, Elephas Bio, and Fortress Biotech (subsidiary); consulting or advisory roles at 2nd.MD, Abbvie, Adept Field Solutions, Aptitude Health, AVEO, Blueprint Partnership, Bristol-Myers Squibb, Catenion, Cello Health, Charles River Associates, Compugen, CurIOS Therapeutics, Daiichi Sankyo, Dedham Group, Defined Health, DLA Piper, Eisai, Elephas Bio, Exelixis, GU Oncology Now, Insight Strategy, Link Cell Therapies, Merck, Neomorph, Nimbus Therapeutics, Octane Co., Pfizer, Schlesinger Associates, Scholar Rock, SignifyMD, Slingshot Insights, Targeted Oncology, and Trinity Group; and research funding from Astra Zeneca and Exelixis. M.S.N. reports consulting or advisory roles at Celgene, Ipsen, Merus, Moderna Therapeutics, and Taiho Pharmaceuticals and research funding from ERYTECH Pharma. R.H.M. reports consulting or advisory roles at Bristol Myers Squibb, IDEAYA Biosciences, Nimbus Therapeutics, and PureTech and research funding from Nimbus Therapeutics and Repare Therapeutics. M.G. reports stock and other ownership in Cota Healthcare; consulting or advisory role at Celularity, Guardant Health, Sanofi; and research funding from Acerta Pharma, Adlai Nortye, Arcus Biosciences, Array BioPharma, Bayer, Bellicum Pharmaceuticals, BMS, Boehringer Ingelheim, Celgene, Checkpoint Therapeutics, Compass Therapeutics, Constellation Pharmaceuticals, Cullinan Oncology, Cyteir, Daiichi Sankyo Company, Eisai, EMD Serono, Erasca Inc, Fate Therapeutics, Georgetown Univ., GlaxoSmithKline, GSB Pharma, Hackensack Meridian Health, Imugene, Incyte, Infinity Pharmaceuticals, ITeos Therapeutics, Janssen, Johnson & Johnson, KSQ Therapeutics, MedImmune, Memorial Sloan Kettering Cancer Center, Merck, Millennium, Mirati Therapeutics, Moderna Therapeutics, NextCure, Nimbus Therapeutics, Pfizer, Pharmacyclics, Rapa Therapeutics, Regeneron, Roche/Genentech, Sanofi, Seagen, Silenseed, Synlogic, Tesaro, Turning Point Therapeutics, Vedanta Biosciences, VelosBio, Verastem, and Vincerx Pharma. S.S. reports stock and ownership interests in Barricade Therapeutics, Beta Cat Pharmaceuticals, Black Canyon Bio, ConverGene, Elevar Therapeutics, HLB, Salarius Pharmaceuticals, and Stingray Therapeutics; honoraria from Array Biopharmaceuticals; consulting or advisory roles at Agastiya Biotech, Barricade Therapeutics, Celularity, Dracen, Elevar Therapeutics, Incyte, Mirati Therapeutics, Novelty Nobility, Processa Pharmaceuticals, Inc, Rappata Therapeutics, and Stemline Therapeutics; research funding from AADI, Adagene, Amal Therapeutics, Celgene, Dracen, Honor Health, Inhibrx, Merck, Nektar, Nimbus Therapeutics, Novartis, Plexxikon, Sirnaomics,

Syndax, Takeda, Tesaro, Toray Industries, and Zai Lab. S.G. reports consulting or advisory roles from Abbvie, ARIAD, Astra Zeneca, Bristol-Myers Squibb, Genentech/Roche, and Pfizer; and received research funding from ARIAD/Takeda, Blueprint Medicines, Genentech/Roche, Merck, and Pfizer. J.P. reports stock and ownership from Oncology Consultants; consulting or advisory roles from Exigent Research Network and research funding from Abbvie, Amgen, Astellas Pharma, AstraZeneca, BerGenBio, Dizal Pharma, EFFECTOR Therapeutics, Epizyme, Genentech/Roche, ImmunityBio, Immunetep, Incyte, Ipsen, Janssen, Kechow Pharma, Lilly, MacroGenics, Mirati Therapeutics, Natera, Novartis, OncoC4, QSAM, Seagen, Sermonix Pharmaceuticals, and Systimmune. T.K.C. reports stock and ownership in Precede Bio, Osel, Tempest Therapeutics, Pionyr, Curesponse, Inndura, Primum, Abalytics Oncology, Bicycle Therapeutics, and Faron Pharmaceuticals; Honorio from HiberCell, Pfizer, Bayer, Novartis, GlaxoSmithKline, Merck, Bristol Myers Squibb, Roche/Genentech, Eisai, Foundation Medicine, AstraZeneca, Exelixis, Promethus, Ipsen, Sanofi/Aventis, Peloton Therapeutics, UpToDate, NCCN, Michael J. Hennessy Associates, Analysis Group, Clinical Care Options, PlatformQ Health, Navinata Health, Harborside Press, ASCO, The New England Journal of Medicine, Lancet Oncology, EMD Serono, Lilly, Tempest Therapeutics, Arcus Biosciences, Alkermes, Gilead Sciences, Scholar Rock, Janssen Oncology, Precede Bio, Aravive, Infinity Pharmaceuticals, ESMO, NiKang Therapeutics, Kanaph Therapeutics, Gilead Sciences, and MashupMD; and research funding from Pfizer, Novartis, Merck, Exelixis, TRACON Pharma, GlaxoSmithKline, Bristol Myers Squibb, AstraZeneca, Peloton Therapeutics, Roche/Genentech, Agensys, Eisai, Takeda, Ipsen, Seattle Genetics/Astellas, Bayer, Roche, Calithera Biosciences, NiKang Therapeutics, Arcus Biosciences, and AVEO. H.E. reports consulting or advisory roles at Bristol-Myers Squibb, Cardinal Health, Cardinal Health, Eisai, Janssen Biotech. B.V.T reports Honorio from Beijing Biostar Pharmaceuticals Co., Ltd., Oncology Education, Total Health Conference; consults or advises for Aadi, Acuta Capital Partners, LLC, Adaptimmune, Advenchen Laboratories, Boxer Capital LLC, Crisper Therapeutics, Daichi Sankyo, Deciphera, Galapagos NV, Hinge Bio, Kronos Bio, Inc., Putnam Associates, Salarius Pharmaceuticals, Inc., and Syneos Health and received research funding from Polaris. R.B. reports Honorio from Cardinal Health; consulting or advisory roles at Bristol-Myers Squibb and AstraZeneca; and received research funding from Bristol-Myers Squibb. G.E., S.R.D., S.N., P.K., and A.S. are current Nimbus Therapeutics employees and shareholders. D.S. reports stock and other ownership interests at Next Oncology and Texas Oncology/US Oncology; received an Honorio from Syneos Health; consulted or advised Nimbus Therapeutics, Revolution Medicines; and received research funding from Abbvie, Acrivon Therapeutics, ADC Therapeutics, Aprea Therapeutics, Ascentage Pharma, Astellas Pharma, Biomea Fusion, BioNTech SE, BJ Bioscience, Boehringer Ingelheim, Bristol-Myers Squibb, Compugen, Day One Biopharmaceuticals, Dicerna, Exelixis, Fate Therapeutics, Gilead Sciences, GlaxoSmithKline, Haihe Pharmaceutical, IconOVir Bio, Immuneering, IMPAC Medical Systems, Incendia Pharmaceuticals AB, Kura Oncology, MediLink, Mirati Therapeutics, ModeX Therapeutics, Monopteros Therapeutics, Navire, NGM Biopharmaceuticals, Nimbus Therapeutics, Novo Nordisk, OBI Pharma, OncoResponse, Pfizer, Revolution Medicines, Step Pharma, Symphogen, Tachyon Therapeutics, Teon Therapeutics, Tylligand Bioscience, Vincerx Pharma/Vincerx Pharma, Vividion Therapeutics, ZielBio, and Zymeworks.

## STAR★METHODS

Detailed methods are provided in the online version of this paper and include the following:

- [KEY RESOURCES TABLE](#)
- [EXPERIMENTAL MODEL AND STUDY PARTICIPANT DETAILS](#)
  - Study design and patients
- [METHOD DETAILS](#)
  - Study treatment and assessments
  - Objectives
  - Pharmacokinetic analysis
  - Whole blood pSLP76 assay
  - Tissue immunofluorescence assays

- Digital spatial profiling
- QUANTIFICATION AND STATISTICAL ANALYSIS
- ADDITIONAL RESOURCES

### SUPPLEMENTAL INFORMATION

Supplemental information can be found online at <https://doi.org/10.1016/j.xcrm.2026.102789>.

Received: July 17, 2025

Revised: November 7, 2025

Accepted: April 9, 2026

### REFERENCES

- Sharma, P., Goswami, S., Raychaudhuri, D., Siddiqui, B.A., Singh, P., Nagarajan, A., Liu, J., Subudhi, S.K., Poon, C., Gant, K.L., et al. (2023). Immune checkpoint therapy current perspectives and future directions. *Cell* **186**, 1652–1669.
- Wei, S.C., Duffy, C.R., and Allison, J.P. (2018). Fundamental mechanisms of immune checkpoint blockade therapy. *Cancer Discov.* **8**, 1069–1086.
- Wang, D.R., Wu, X.L., and Sun, Y.L. (2022). Therapeutic targets and biomarkers of tumor immunotherapy: response versus non-response. *Signal Transduct. Target. Ther.* **7**, 331.
- Wang, S.L., and Chan, T.A. (2025). Navigating established and emerging biomarkers for immune checkpoint inhibitor therapy. *Cancer Cell* **43**, 641–664.
- Haslam, A., and Prasad, V. (2019). Estimation of the percentage of US patients with cancer who are eligible for and respond to checkpoint inhibitor immunotherapy drugs. *JAMA Netw. Open* **2**, e192535.
- Topalian, S.L., Hodi, F.S., Brahmer, J.R., Gettinger, S.N., Smith, D.C., McDermott, D.F., Powderly, J.D., Sosman, J.A., Atkins, M.B., Leming, P.D., et al. (2019). Five-year survival and correlates among patients with advanced melanoma, renal cell carcinoma, or non-small cell lung cancer treated with nivolumab. *JAMA Oncol.* **5**, 1411–1420.
- Pons-Tostivint, E., Latouche, A., Vaflard, P., Ricci, F., Loirat, D., Hescot, S., Sablin, M.P., Rouzier, R., Kamal, M., Morel, C., et al. (2019). Comparative analysis of durable responses on immune checkpoint inhibitors versus other systemic therapies: a pooled analysis of phase III trials. *JCO Precis. Oncol.* **3**, 1–10.
- Yarchoan, M., Hopkins, A., and Jaffee, E.M. (2017). Tumor mutational burden and response rate to PD-1 inhibition. *N. Engl. J. Med.* **377**, 2500–2501.
- Anderson, K.G., Braun, D.A., Buqué, A., Gitto, S.B., Guerriero, J.L., Horton, B., Keenan, B.P., Kim, T.S., Overacre-Delgoffe, A., Ruella, M., et al. (2023). Leveraging immune resistance archetypes in solid cancer to inform next-generation anticancer therapies. *J. Immunother. Cancer* **11**, e006533.
- Motzer, R.J., Tannir, N.M., McDermott, D.F., Arén Frontera, O., Melichar, B., Choueiri, T.K., Plimack, E.R., Barthélémy, P., Porta, C., George, S., et al. (2018). Nivolumab plus ipilimumab versus sunitinib in advanced renal-cell carcinoma. *N. Engl. J. Med.* **378**, 1277–1290.
- Rini, B.I., Plimack, E.R., Stus, V., Gafanov, R., Hawkins, R., Nosov, D., Pouliot, F., Alekseev, B., Soulières, D., Melichar, B., et al. (2019). Pembrolizumab plus axitinib versus sunitinib for advanced renal-cell carcinoma. *N. Engl. J. Med.* **380**, 1116–1127.
- Choueiri, T.K., Powles, T., Burotto, M., Escudier, B., Bourlon, M.T., Zurawski, B., Oyervides Juárez, V.M., Hsieh, J.J., Basso, U., Shah, A.Y., et al. (2021). Nivolumab plus cabozantinib versus sunitinib for advanced renal-cell carcinoma. *N. Engl. J. Med.* **384**, 829–841.
- Motzer, R., Alekseev, B., Rha, S.Y., Porta, C., Eto, M., Powles, T., Grünwald, V., Hutson, T.E., Kopyltsov, E., Méndez-Vidal, M.J., et al. (2021). Lenvatinib plus pembrolizumab or everolimus for advanced renal cell carcinoma. *N. Engl. J. Med.* **384**, 1289–1300.
- Karasarides, M., Cogdill, A.P., Robbins, P.B., Bowden, M., Burton, E.M., Butterfield, L.H., Cesano, A., Hammer, C., Haymaker, C.L., Horak, C.E., et al. (2022). Hallmarks of resistance to immune-checkpoint inhibitors. *Cancer Immunol. Res.* **10**, 372–383.
- Jenkins, R.W., Barbie, D.A., and Flaherty, K.T. (2018). Mechanisms of resistance to immune checkpoint inhibitors. *Br. J. Cancer* **118**, 9–16.
- Sharma, P., Hu-Lieskovan, S., Wargo, J.A., and Ribas, A. (2017). Primary, adaptive, and acquired resistance to cancer immunotherapy. *Cell* **168**, 707–723.
- Hiltbrunner, S., Cords, L., Kasser, S., Nüesch-Noël, S., Kreutzer, S., Toussein, N.C., Grob, L., Opitz, I., Messerli, M., Früh, M., et al. (2023). Acquired resistance to anti-PD1 therapy in patients with NSCLC associates with immunosuppressive T cell phenotype. *Nat. Commun.* **14**, 5184.
- Morad, G., Helmink, B.A., Sharma, P., and Wargo, J.A. (2021). Hallmarks of response, resistance, and toxicity to immune checkpoint blockade. *Cell* **184**, 5309–5337.
- Sawasdikosol, S., and Burakoff, S. (2020). A perspective on HPK1 as a novel immuno-oncology drug target. *eLife* **9**, e55122.
- Chuang, H.-C., Wang, X., and Tan, T.H. (2016). Map4k family kinases in immunity and inflammation. *Adv. Immunol.* **129**, 277–314.
- Hernandez, S., Qing, J., Thibodeau, R.H., Du, X., Park, S., Lee, H.M., Xu, M., Oh, S., Navarro, A., Roose-Girma, M., et al. (2018). The kinase activity of hematopoietic progenitor kinase 1 is essential for the regulation of T cell function. *Cell Rep.* **25**, 80–94.
- Nager, A., Schaer, D., Gallego, R., Hendrickson, E., Timofeevski, S., Li, M., Côté, B., Halcomb, R., Greenwood, J., Kozłowski, J., et al. (2022). 1367 A highly-selective HPK1 inhibitor enhances T cell receptor signaling and T cell activation potential, increasing antigen recognition and efficacy of PD-1 therapy. *J. Immunother. Cancer* **10**, A1418.
- Zhou, L., Wang, T., Zhang, K., Zhang, X., and Jiang, S. (2022). The development of small-molecule inhibitors targeting HPK1. *Eur. J. Med. Chem.* **244**, 114819.
- Di Bartolo, V., Montagne, B., Salek, M., Jungwirth, B., Carrette, F., Fourtane, J., Sol-Foulon, N., Michel, F., Schwartz, O., Lehmann, W.D., et al. (2007). A novel pathway down-modulating T cell activation involves HPK1-dependent recruitment of 14-3-3 proteins on SLP-76. *J. Exp. Med.* **204**, 681–691.
- Lasserre, R., Cuche, C., Blecher-Gonen, R., Libman, E., Biquand, E., Danckaert, A., Yablonski, D., Alcover, A., and Di Bartolo, V. (2011). Release of serine/threonine-phosphorylated adaptors from signaling microclusters down-regulates T cell activation. *J. Cell Biol.* **195**, 839–853.
- Sauer, K., Liou, J., Singh, S.B., Yablonski, D., Weiss, A., and Perlmutter, R.M. (2001). Hematopoietic progenitor kinase 1 associates physically and functionally with the adaptor proteins B cell linker protein and SLP-76 in lymphocytes. *J. Biol. Chem.* **276**, 45207–45216.
- Wang, X., Li, J.-P., Kuo, H.-K., Chiu, L.-L., Dement, G.A., Lan, J.-L., Chen, D.-Y., Yang, C.-Y., Hu, H., and Tan, T.-H. (2012). Down-regulation of B cell receptor signaling by hematopoietic progenitor kinase 1 (HPK1)-mediated phosphorylation and ubiquitination of activated B cell linker protein (BLNK). *J. Biol. Chem.* **287**, 11037–11048.
- Alzabin, S., Bhardwaj, N., Kiefer, F., Sawasdikosol, S., and Burakoff, S. (2009). Hematopoietic progenitor kinase 1 is a negative regulator of dendritic cell activation. *J. Immunol.* **182**, 6187–6194.
- Alzabin, S., Pyarajan, S., Yee, H., Kiefer, F., Suzuki, A., Burakoff, S., and Sawasdikosol, S. (2010). Hematopoietic progenitor kinase 1 is a critical component of prostaglandin E2-mediated suppression of the anti-tumor immune response. *Cancer Immunol. Immunother.* **59**, 419–429.
- Liu, J., Curtin, J., You, D., Hillerman, S., Li-Wang, B., Eraslan, R., Xie, J., Swanson, J., Ho, C.P., Oppenheimer, S., et al. (2019). Critical role of kinase activity of hematopoietic progenitor kinase 1 in anti-tumor immune surveillance. *PLoS One* **14**, e0212670.

31. Si, J., Wang, X., Li, M., Xu, Y., Jiang, L., Wang, Y., Pan, Q., Zhu, X., Zhang, L., Liu, Z., et al. (2020). Hematopoietic progenitor kinase 1 (HPK1) mediates T cell dysfunction and is a druggable target for T cell-based immunotherapies. *Cancer Cell* *38*, 551–566.e9.
32. Chuang, H.-C., Lan, J.-L., Chen, D.-Y., Yang, C.-Y., Chen, Y.-M., Li, J.-P., Huang, C.-Y., Liu, P.-E., Wang, X., and Tan, T.-H. (2011). The kinase GLK controls autoimmunity and NF- $\kappa$ B signaling by activating the kinase PKC- $\theta$  in T cells. *Nat. Immunol.* *12*, 1113–1118.
33. Kaila, N. (2024). Discovery of NDI-101150, a highly potent and selective HPK1 inhibitor for the treatment of cancer, through structure-based drug design. *Am. Chem. Soc.*
34. Ciccone, D., Kuo, F.-S., Boiko, S., Daigle, S., Klinger, A., Peterson, A., Hutt, J., Wang, Q., Nichols, K., Ward, C., et al. (2023). NDI-101150 is a potent and highly selective hematopoietic progenitor kinase 1 (HPK1) inhibitor that promotes a robust and broad anti-tumor immune response. *J. Immunother. Cancer* *11*, A1494.
35. Papadopoulos, K.P., Fu, S., Hamilton, E., Laurie, S.A., Spira, A., Wang, J., Ma, W.W., Hamid, O., Spreafico, A., Sharma, S., et al. (2023). 741 TWT-101: A first-in-clinic study of CFI-402411, a hematopoietic progenitor kinase-1 (HPK1) inhibitor, as single agent or combined with pembrolizumab in subjects with advanced solid malignancies. *J. Immunother. Cancer* *11*, A835.
36. Deva, S., Zhou, C., Bishnoi, S.K., Lau, P.K.H., Tran, B., Ba, Y., Galsky, M.D., Wang, Y., Zhang, Y., Luo, S., et al. (2024). A first-in-human phase 1a dose-escalation study of BGB-15025 (HPK1 inhibitor) as monotherapy and in combination with tislelizumab (TIS; anti-PD-1 antibody) in patients (pts) with advanced solid tumors. *J. Clin. Oncol.* *42*, 2585.
37. Choueiri, T.K., Albiges, L., Barthélémy, P., Iacovelli, R., Emambux, S., Molina-Cerrillo, J., Garmez, B., Barata, P., Basu, A., Bourlon, M.T., et al. (2024). Tivozanib plus nivolumab versus tivozanib monotherapy in patients with renal cell carcinoma following an immune checkpoint inhibitor: results of the phase 3 TiNivo-2 study. *Lancet* *404*, 1309–1320.
38. Pal, S.K., Albiges, L., Tomczak, P., Suárez, C., Voss, M.H., de Velasco, G., Chahoud, J., Mochalova, A., Procopio, G., Mahammed, H., et al. (2023). Atezolizumab plus cabozantinib versus cabozantinib monotherapy for patients with renal cell carcinoma after progression with previous immune checkpoint inhibitor treatment (CONTACT-03): a multicentre, randomised, open-label, phase 3 trial. *Lancet* *402*, 185–195.
39. Merck & Eisai. (2025). Merck and Eisai announce WELIREG (belzutifan) plus LENVIMA (lenvatinib) met primary endpoint of progression-free survival (PFS) in certain previously treated patients with advanced renal cell carcinoma. Press release, October 28, 2025. Available at: [https://s2.q4cdn.com/584635680/files/doc\\_news/Merck-and-Eisai-Announce-WE-LIREG-belzutifan-Plus-LENVIMA-lenvatinib-Met-Primary-Endpoint-of-Progression-Free-Survival-PFS-in-Certain-VLW1Q.pdf](https://s2.q4cdn.com/584635680/files/doc_news/Merck-and-Eisai-Announce-WE-LIREG-belzutifan-Plus-LENVIMA-lenvatinib-Met-Primary-Endpoint-of-Progression-Free-Survival-PFS-in-Certain-VLW1Q.pdf).
40. Merck. (2025). Merck Announces KEYTRUDA (Pembrolizumab) Plus WELIREG (Belzutifan) Met Primary Endpoint of Disease-free Survival (DFS) in Certain Patients with Clear Cell Renal Cell Carcinoma (RCC) Following Nephrectomy. Press release, October 28, 2025. Available at: [https://s2.q4cdn.com/584635680/files/doc\\_news/Merck-Announces-KEYTRUDA-pembrolizumab-Plus-WELIREG-belzutifan-Met-Primary-Endpoint-of-Disease-Free-Survival-DFS-in-Certain-Patients-8VRDG.pdf](https://s2.q4cdn.com/584635680/files/doc_news/Merck-Announces-KEYTRUDA-pembrolizumab-Plus-WELIREG-belzutifan-Met-Primary-Endpoint-of-Disease-Free-Survival-DFS-in-Certain-Patients-8VRDG.pdf).
41. Davis, E.J., Martin-Liberal, J., Kristeleit, R., Cho, D.C., Blagden, S.P., Berthold, D., Cardin, D.B., Vieito, M., O'Neil, B.H., Hari Dass, P., et al. (2022). First-in-human phase I/II, open-label study of the anti-OX40 agonist INCAGN01949 in patients with advanced solid tumors. *J. Immunother. Cancer* *10*, e004235.
42. Rousseau, A., Parisi, C., and Barlesi, F. (2023). Anti-TIGIT therapies for solid tumors: a systematic review. *ESMO Open* *8*, 101184.
43. KEYTRUDA (pembrolizumab) prescribing information. (2025). Merck & Co., Inc., Rahway, NJ, USA; revised April 2025. Available at: [https://www.merck.com/product/usa/pi\\_circulars/k/keytruda/keytruda\\_pi.pdf](https://www.merck.com/product/usa/pi_circulars/k/keytruda/keytruda_pi.pdf).
44. Cardenes, R., Wood, D., Schulze, M., Lee, J., and Rognoni, L. (2024). UtiAnalyzer.AI: an automatic and robust AI-driven tool for the quantification of multiplex immunofluorescence whole slide images. *Cancer Res.* *84*, A4932.
45. Szabo, P.A., Levitin, H.M., Miron, M., Snyder, M.E., Senda, T., Yuan, J., Cheng, Y.L., Bush, E.C., Dogra, P., Thapa, P., et al. (2019). Single-cell transcriptomics of human T cells reveals tissue and activation signatures in health and disease. *Nat. Commun.* *10*, 4706.
46. Finotello, F., Mayer, C., Plattner, C., Laschober, G., Rieder, D., Hackl, H., Krogsdam, A., Loncova, Z., Posch, W., Wifflingseder, D., et al. (2019). Correction to: Molecular and pharmacological modulators of the tumor immune contexture revealed by deconvolution of RNA-seq data. *Genome Med.* *11*, 50.
47. Danaher, P., Kim, Y., Nelson, B., Griswold, M., Yang, Z., Piazza, E., Beechem, J.M., and Warren, S. (2022). Advances in mixed cell deconvolution enable quantification of cell types in spatial transcriptomic data. *Nat. Commun.* *13*, 385.

STAR★METHODS

KEY RESOURCES TABLE

REAGENT or RESOURCE	SOURCE	IDENTIFIER
<b>Antibodies</b>		
Anti-CD45	BD Biosciences	RRID:AB_2869519
Anti-CD3	BioLegend	RRID:AB_2904327
Anti-CD4	BioLegend	RRID:AB_10965645
Anti-CD8	BD Biosciences	Cat# 563677
Phospo-SLP76 (S376)	Cell Signaling Technologies	Cat# 76143
Anti-human CD3 Stimulation Agent	BioLegend	RRID:AB_11150592
Anti-human CD28 Stimulation Agent	BioLegend	RRID:AB_11148949
Goat anti-mouse IgG	ThermoFisher (Invitrogen)	Cat# 31160
BD PhosFlow Lyse/Fix Buffer	BD Biosciences	RRID:AB_2869117
BD PhosFlow Perm/Wash Buffer	BD Biosciences	RRID:AB_2869104
Human TruStain FcX	BioLegend	RRID:AB_2818986
Anti-KI-67 Clone SP6	Abcam	RRID:AB_2924695
Anti- Granzyme B Clone EPR8260	Abcam	Cat# ab226162
Anti-LAG3 Clone EPR20261	Abcam	Cat# ab227579
Anti-HLA-DR Clone TAL1B5	Abcam	RRID:AB_3492081
Anit-CD8 Clone C8/144B	Biocare	Cat# 3160
Anti-PD-1 Clone CAL20	Abcam	Cat# ab251613
Anti-FoxP3 Clone 236A/E7	ThermoFisher (Invitrogen)	Cat# 14-4777
Anti-CD11c Clone EP1347Y	Abcam	RRID:AB_2864379
Anti-CD3 Clone BC33	Biocare	Cat# 3170
Anti-CD4 Clone SP35	Abcam	Cat# ab238798
Anti-CD20 Clone L26	ThermoFisher (Invitrogen)	Cat# 14-0202
Anti-CK Clone AE1/AE3	Fortis Life Sciences	Cat# A500-019A
Anti-pSLP76 (Ser376) [E3G9U]-T91 ISP	Cell Signaling Technology	Cat# 10190SF
<b>Biological samples</b>		
Human Blood	Patients in this study	N/A
Human tumor tissue samples	Patients in this study	N/A
<b>Software and algorithms</b>		
Phoenix® WinNonlin® v.8.5.	Certara	N/A
BD LSRFortessa™ Cell Analyzer	BD Biosciences	Cat# 647800L
BD FACSDiva™ v9.0	BD Biosciences	N/A
FlowCut® v1.0	CellCarta	N/A
CellEngine® v6.1	CellCarta	N/A
Ultivue's UltiStacker Software	Ultivue	N/A
<b>Other</b>		
Antibody Diluent	Ultivue	Cat# 40390
Pre-Amplification Mix	Ultivue	Cat# 40039
Amplification Solution	Ultivue	Cat# 40030
Bond Wash Solution	Leica Biosystems	Cat# AR9590
Bond ER2 Solution	Leica Biosystems	Cat# AR9640

## EXPERIMENTAL MODEL AND STUDY PARTICIPANT DETAILS

### Study design and patients

NDI-101150 was tested in a human, multicenter, open-label, Phase 1/2 trial as a monotherapy or in combination with pembrolizumab in patients with advanced solid tumors who were ineligible for or refractory to standard-of-care therapy. Fifty seven percent of the participants were male with a median age of 66 years (range: 21–90). The dose-escalation phase of the study included patients with histologically or cytologically confirmed advanced or metastatic solid tumors for whom no standard therapies were available or whose tumors were refractory to standard therapy. Patients with measurable or non-measurable disease were allowed in the dose escalation phase of the study. In the dose expansion phase, patients with histologically or cytologically confirmed advanced or metastatic RCC, NSCLC, and G/GEJ for which no standard therapies were available or were refractory to standard therapy were included. Patients were required to have measurable disease using Response Evaluation Criteria In Solid Tumors version 1.1 (RECIST v1.1) to enroll in the dose expansion phase of the study.

The study protocol was reviewed and approved by an independent ethics committee and relevant regulatory authority in the United States of America. The full study protocol can be found as supplementary information ([Data S1](#)). The study design and execution of the study adhered to all relevant regulations concerning the use of human study participants. All patients or their legal representatives provided written informed consent before participating in the study.

## METHOD DETAILS

### Study treatment and assessments

In patients who received NDI-101150 monotherapy, NDI-101150 was administered orally in capsule form every day continuously in 4-week cycles (28 days) at each of the pre-specified doses of 50 mg, 100 mg, 140 mg, 150 mg, and 200 mg. In patients who received the combination therapy, NDI-101150 was administered orally in capsule form continuously once daily in 3-week cycles (21 days) at 50 mg or 100 mg doses, and pembrolizumab was administered intravenously at 200 mg dose every 3 weeks (Q3W) following the pembrolizumab USPI.<sup>43</sup> On days when NDI-101150 and pembrolizumab were co-administered, NDI-101150 was administered first and observed for at least 30 min prior to administration of pembrolizumab. Each dose of pembrolizumab was administered at the study center. Study treatment was continued until occurrence of any of the following events which led to permanent discontinuation of study drug, including occurrence of disease progression, unacceptable toxicity, withdrawal of consent by patient, withdrawal of the patient by the investigator, death, start of new systemic anti-cancer treatment, or termination of the study by Sponsor.

Using a standard 3 + 3 design, DLTs were evaluated during the first 4 weeks (28 days) of NDI-101150 monotherapy escalation cohorts, or during the first 6 weeks (42 days) of NDI-101150 and pembrolizumab combination escalation cohorts. The DLTs were evaluated using the NCI CTCAE Criteria v5.0.

Tumor response was evaluated by the study investigators according to RECIST v1.1. The response was categorized as complete response (CR), partial response (PR), stable disease (SD), progressive disease (PD), and non-evaluable (NE). Radiographic tumor assessments (via computed tomography) were conducted approximately every 8 weeks ( $\pm 7$  days) from Cycle 1 Day 1 (C1D1) dosing in the monotherapy cohorts or every 9 weeks ( $\pm 7$  days) from C1D1 dosing for the NDI-101150 and pembrolizumab combination therapy cohorts until discontinuation of study treatment or withdrawal of consent, whichever occurred first. The CR and PR were confirmed with at least one subsequent imaging scan.

### Objectives

For the dose escalation phase, the primary endpoint was determination of DLT associated with NDI-101150 monotherapy or in combination with pembrolizumab in all solid tumor patients. For the dose expansion phase, the primary endpoint was evaluation of ORR as per RECISTv1.1 in patients with RCC, NSCLC, and G/GEJ. Objective response rate was a secondary endpoint for dose escalation cohorts, while secondary endpoints for both dose escalation and expansion phases included assessment of incidence of adverse events (AEs), serious AEs (SAEs), clinical benefit rate (CBR), duration of response (DOR), time to response (TTR), progression free survival (PFS), overall survival (OS), and pharmacokinetic (PK) profile associated with NDI-101150 monotherapy or in combination with pembrolizumab. The CBR was defined as  $CR + PR + SD \geq 6$  months, while disease control rate was defined as  $CR + PR + SD$  of any duration.

### Pharmacokinetic analysis

NDI-101150 plasma concentrations were analyzed on Cycle 1 Days 1 and 15, and/or Cycle 2 Day 1 pre-dose, and at 0.5, 1, 2, 3, 4, 6, 8, and 24 h post dose. Additional pre-dose samples were collected on Cycle 1 Day 22, Cycle 2 Day 15, and Cycle 3 Day 1.

For the pilot food-effect cohort, on Cycle 0 Day 1, following the 2-h fast pre-dose, patients were given a high-fat and high-calorie meal along with 240 mL of water (fed condition), approximately 30 min before administration of NDI-101150. On Cycle 1 Day 1 (and all other days of treatment), patients fasted for 2 h taking NDI-101150 (modified fasted condition). Blood samples for PK were collected at pre-dose, 0.5, 1, 2, 3, 4, 6, 8, 24, 48 (Cycle 0 only), and 72 (Cycle 0 only) hours post-dose.

Plasma concentrations of NDI-101150 were determined, using a validated high-performance liquid chromatographic-tandem mass spectrometry (LC-MS/MS) method. Briefly, plasma samples were fortified with an internal standard (NDI-101150-d6) and

extracted by protein precipitation. Reversed-phase high-pressure liquid chromatography (HPLC) separation was achieved with an ACE 3 C18 column (50 × 2.1mm, 3.0 μm). MS/MS detection was set at mass transitions of  $m/z$  487.2→386.1 for NDI-101150 in TurbolonSpray positive mode. The standard curve had a dynamic range of 1.00–1000 ng/mL.

Key PK parameters evaluated by non-compartmental analysis (NCA; Phoenix WinNonlin, Certara) included maximum observed plasma concentration ( $C_{max}$ ), time of maximum plasma concentration ( $T_{max}$ ), area under the plasma concentration-time curve from time zero to 24 h post-dose ( $AUC_{0-24h}$ ), terminal elimination half-life ( $t_{1/2}$ ), and accumulation ratio (RA).

### Whole blood pSLP76 assay

Baseline (pre-dose Cycle 1 Day 1) samples were compared to on-treatment samples taken after dosing on Cycle 1 Days 1 and 15 at 2, and 4 h, and pre-dose samples on Cycle 1 Days 2, 8, 15, and 21. Following collection in sodium heparin vacutainers, blood was shipped overnight to a third-party vendor (CellCarta) and processed. Briefly, 90 μLs of whole blood was stimulated with anti-CD3/anti-CD28 or phosphate buffered saline (unstimulated control). Following stimulation, cells were lysed and fixed, then frozen as cell pellets at  $-80^{\circ}\text{C}$  for storage. For analysis, both unstimulated and stimulated frozen cell pellets samples were thawed. The cells were then blocked to reduce nonspecific binding, followed by surface staining. Next, cell permeabilization followed by intracellular staining of pSLP76 (Serine 376) was performed. Finally, samples were acquired on a BD LSRFortessa cytometer for analysis. Flow analysis was performed utilizing a standard gating procedure (Figure S5) and percent of baseline was analyzed for the median fluorescence intensity of the CD3<sup>+</sup>CD8<sup>+</sup>pSLP76<sup>+</sup> population. Samples were considered outside of stability if they were received greater than three days following collection and/or processed more than four days after collection. Following staining samples were considered stable for 24 h at  $2^{\circ}\text{C}$ – $8^{\circ}\text{C}$  or frozen for <5 weeks (35 days). Anything beyond this was considered an assay failure.

### Tissue immunofluorescence assays

Tumor tissue biopsies were considered optional during the dose escalation phase of the study, while in dose expansion, biopsies were mandatory at baseline (archival pre-dose was acceptable with medical monitor approval) and on treatment (Day 28 ± 7 days). 4-micron formalin-fixed paraffin-embedded tumor tissue sections from pre- and on-treatment patient samples were evaluated with Ultivue's InSituPlex. The multiplex immunofluorescence assays used custom 12-plex (CD3, CD4, CD8, CD11c, CD20, FoxP3, GrzB, HLA-DR, Ki-67, Lag3, pan-CK, and PD-1) and 2-plex (CD3, pSLP76) U-VUE panels. Images were quality controlled for necrotic areas of tissue as well as edge staining, folds, tears, blurred and/or misaligned areas, and other artifacts excluded as needed throughout. Large areas of autofluorescence in red cells and elastic fibers were also excluded from analysis as needed to reduce false positives. Standard image analysis was performed as previously outlined.<sup>44</sup> For pSLP76 analysis, tumor tissue levels were calculated from 2-Plex immunofluorescence as CD3<sup>+</sup>pSLP76<sup>+</sup> densities normalized to total CD3<sup>+</sup> densities. Likewise, 12-Plex analyses were normalized to the parental cell type (e.g., CD3<sup>+</sup>CD8<sup>+</sup>GrzB<sup>+</sup>, densities were normalized to CD3<sup>+</sup>CD8<sup>+</sup> densities).

### Digital spatial profiling

Digital spatial profiling (DSP) experiments were performed according to the Nanostring GeoMx-NGS DSP Instrument Manual. Briefly, FFPE tissues from pre- and on-treatment biopsies were analyzed for spatially resolved profiling of the whole transcriptome atlas using NanoString's GeoMx DSP platform at Canopy Biosciences, Hayward, CA (Bruker Nano Inc, Billerica, MA, USA). Slides were imaged in the Cy5/666 nm channel to detect CD45 (Cell Signaling Technology, 19744). Photo-cleavable RNA probes were released from CD45 positive and CD45 negative cellular segments by UV light and sequenced using an NGS readout (Illumina NovaSeq X Plus system). For each 4-micron slide, 10 regions of interest (5 regions corresponded to tumor areas, and 5 regions corresponded to non-tumor areas) of ~450,000 mm<sup>2</sup> as defined by a pathologist were selected and segmented into CD45<sup>+/−</sup> cells. FASTQ files were processed using the Nanostring GeoMx NGS Pipeline v2.2. For analysis, NGS counts were processed as recommended by Nanostring. Target counts were normalized with a third quartile normalization. Targets with 1% segments above the limit of quantification were kept. Linear Mixed Effects models were used to characterize and derive  $p$ -values for differences in expression between experimental groups. Differential gene expression and unsupervised clustering were performed using the GeoMx Data Analysis suite. Gene set enrichment analysis (GSEA) was performed using the fGSEA package from Bioconductor on log<sub>2</sub> fold-change values between experimental groups. Immune gene sets were obtained from published datasets.<sup>45–47</sup>

## QUANTIFICATION AND STATISTICAL ANALYSIS

Clinical data processing, tabulation of descriptive statistics, calculation of inferential statistics and graphical representations except for PK parameter estimation and translational analyses utilized SAS (release 9.4 or higher). A detailed summary of statistical analyses are outlined in the statistical analysis plan (Data S1).

## ADDITIONAL RESOURCES

The study was registered with [ClinicalTrials.gov](https://clinicaltrials.gov), number NCT05128487.